STRUCTURE ORIENTED 3D ROUGHNESS EVALUATION WITH OPTICAL PROFILERS

Arnim Weidner
IMR, University of Hannover, Nienburger Str. 17, +49-511-762-5816, -3234, weidner@imr.uni-hannover.de
Jörg Seewig
IMR, University of Hannover, Nienburger Str. 17, +49-511-762-4286, -3234, seewig@imr.uni-hannover.de
Eduard Reithmeier
IMR, University of Hannover, Nienburger Str. 17, +49-511-762-3334, -3234, sekretariat@imr.uni-hannover.de

Abstract :

Modern cylinder liner manufacturing processes like MMC casting, laser honing and laser exposure allow a design of cylinder liner surfaces to meet common development goals like less air pollution and reduced fuel and oil consumption. These goals are reached by aimed insertion of function relevant structures in the micrometer scale into the surface. Because of this function relevant structures the commonly used 2D roughness parameters like Ra and Rz provide only a limited description of the functional behaviour of these surfaces. To describe these designed surfaces it is necessary to extend the roughness evaluation into the third dimension: $z=z(x,y)$.

This paper evaluates optical surface measurement technologies like white light interferometry and confocal microscopes with respect to measure surface roughness in three dimensions. It shows characteristic differences between data measured by tactile and optical profilers. Based on these data this paper proposes guidelines to develop more repeatable and stable but still selective 3D roughness parameters. With the structure oriented 3D roughness evaluation developed at the University of Hannover the advantages of this guidelines are shown by evaluating tactile and optical measured surfaces with comparable results.

Key words: robust 3D roughness evaluation, structural parameter, topography, optical and tactile roughness measurement, round robin, optical profiler, white light interferometer, confocal microscope

1 Introduction

The commonly used 2D roughness evaluation could not describe the additional functions of modern designed surfaces. These surfaces provide their tribological functionality through spatially distributed structures in the roughness scale which makes it necessary to measure and evaluate them in three dimensions.
The established and well-known tactile profilers are too slow for industrial 3D measurements. With optical profilers a 3D roughness measurement can be carried out in an acceptable time. But these optical profilers show some systematic differences from the common tactile profilers which makes it impossible to simply use the standardised roughness parameters according to ISO 4287.
With a round robin test of optical profilers an applicability of optical profilers for roughness measurements was evaluated. Furthermore, some guidelines for adapted roughness parameters were developed. This paper introduces some of the results of this round robin test.

2 Round robin test of optical profilers

To test the suitability of optical measurement systems for a 3D roughness evaluation a round robin test of state of the art optical profilers was carried out. In this round robin test a wide range of optical systems were included: white light interferometers, white light- and laser scanning confocal microscopes and chromatic point sensors. Pfeifer [1] and Schwenke [2] give a comprehensive overview of optical sensors for roughness measurements.

To test the optical profilers a set of real world samples mostly cylinder liners was chosen. The samples were selected to have surfaces which in the past showed some critical behaviour when measured with optical systems. These samples included surfaces with different materials, surfaces with steep edges in a height range from a fraction to a multiple of the illumination wavelength, surfaces with a nano/micro roughness, one surface with a very deep hole and one surface with very high local intensity contrasts. Further a reference mirror was included to test the noise sensitivity and linearity of the optical systems. For these tests the VDI2655-1 [3] was taken into account.

Fig.1: *samples of cylinder liner surfaces with characteristic structures: a) MMC (metal matrix composites) casted surface, b) laser exposed surface, c) laser honed surface.*

The roughness samples were prepared with a reference marker to always find the same area on the surface. Before measuring the surfaces with the optical profilers SEM pictures were taken to get an overview of the region of interest. The SEM pictures were used as a kind of map to find the interesting structures. To get a tactile reference some of the samples were measured at the Physikalisch Technische Bundesanstalt (PTB), Braunschweig with a long range SPM: M-LRSPM [4].
With the samples the manufacturers of the optical systems were visited. To realise an optimal measurement the samples were measured by personal of the manufacturer. The operators had a look at the samples and decided which optical setup to use to achieve an optimal measurement result. The measurement data was saved as raw data without any post processing: no alignment, no filtering, no interpolation of missing points.
The evaluation of the measurement data was carried out with the structure oriented 3D roughness evaluation [5]. Within the measurement areas some significant structures were chosen. With a novel detection technique [6] these structures were separated and described with structural parameters. The structural parameters of the optical profilers were compared against the tactile reference.

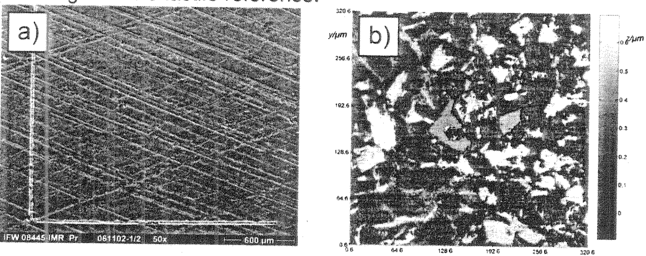

Fig.2: *a) reference marker to measure the same surface area, b) structures used for a structure oriented evaluation.*

3 Systematic differences of optical roughness measurements

Three systematic main differences compared to tactile profilers occurred by measuring roughness with optical systems: missing points, batwings and small measuring fields. In addition to these three main problems optical profilers showed some smaller drawbacks which could be handled with adapted setups (closed loop drives and stages).

10th International Conference Metrology and Properties of Engineering Surfaces Saint Etienne, 4-7 July 2005

3.1 Missing points

Optical profilers use light (photons) to collect information about the surface. Every time a significant amount of photons can get from the light source to the surface and back to the light sensor surface information can be provided. If this is impossible or some unexpected changes to the photons (wavelength, phase) occur, no information of the surface can be extracted. If an optical profiler has the capability to notice this information losses a missing point is generated. So a missing point contains the information: the measurement system did approach its physical limit. Most of the missing points appeared for two reasons: steep edges and high local reflectivity contrasts.

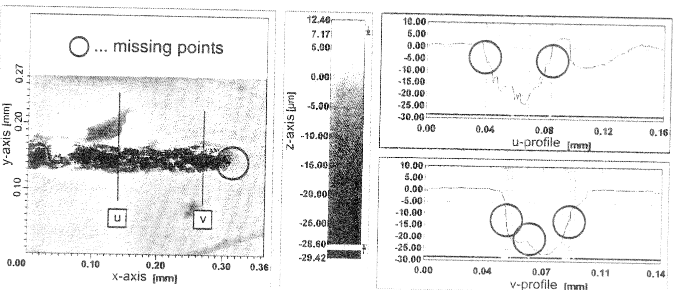

Fig.3: *laser hole of a laser honed surface, with gradient angles of the steep edges up to 89°: a) gray coded height plot, b) profile of the laser hole.*

The steepness of an edge is defined with the numerical aperture of a microscope objective. In other words, if the light reflected by the edge misses the objective, it can not be projected on the CCD sensor and no information can be extracted. To avoid missing points due to steep edges objectives with higher numerical apertures could be used.
As a second reason of missing points high local reflectivity contrasts can exceed the dynamic range of the light sensitive sensors (CCDs). With this high contrast surfaces a compromise between measuring dark and bright points has to be chosen.

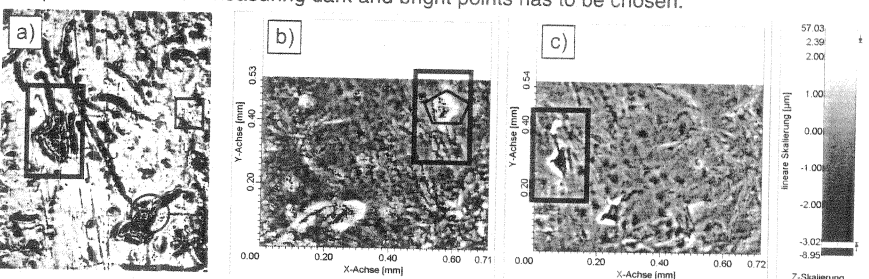

Fig.4: *graphite accumulation of a laser exposed grey casted iron surface: a) reflection image: maximum reflected intensity of the surface, b) surface measured with a white light interferometer with one intensity, c) same optical setup like b) but surface measured with two intensities.*

In contrast to confocal microscopes, the two optical paths of an interferometer pose more difficulties with high contrast surfaces. With a constant source intensity the reference path is providing a constant reference intensity against which the varying surface intensity is

compared. The signal to noise ratio (SNR) of an interference figure is lowered the more the intensities of both optical paths differ. An adaptation of the reference mirror reflectivity and successive measurements with two or more source intensities [7] can rise the SNR which leads to less missing points (Fig. 4c). Furthermore, an extension of the dynamic range of the light sensor could improve the measuring of high contrast surfaces. With such an adapted interferometer the amount of missing points due to high contrast surfaces turned out to be comparable to confocal systems.

3.2 Batwings

Batwings are artefacts which occur mostly on steep edges like missing points, too [8]. The optical profiler does not recognize the steep edge as a missing point but it calculates a height information which does not represent the actual height.

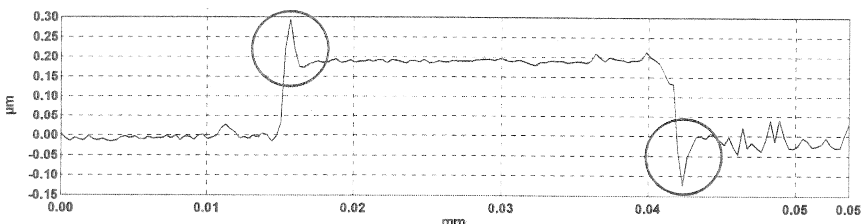

Fig.5: *step height standard with batwings at the edges.*

For clearly separated structures like MST/MEMS devices the batwing artefacts can be handled very good with a subsequent filtering of the measured surface. Rough surfaces turned out to be more difficult. Because of the roughness nearly everywhere on the surface small steep edges can occur. These small steep edges lead to an over- or underestimation of the height of these points and as a result to an amplification of a small roughness through batwing artefacts.

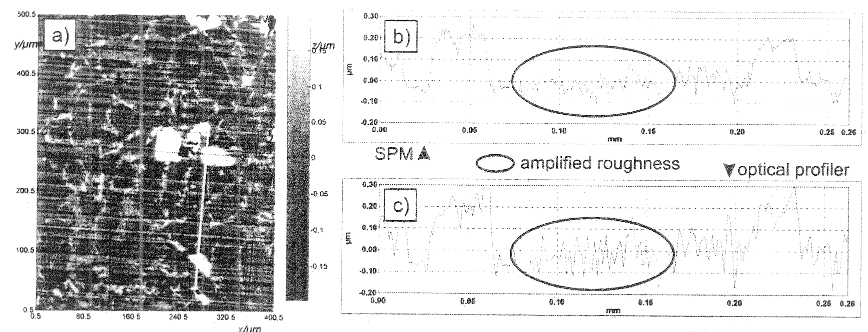

Fig.6: *amplified roughness through batwing artefacts: a) grey coded height plot of the topography, b) profile measured with the M-LRSPM, c) same profile as b) measured with an optical profiler with batwing artefacts.*

Batwings have to be avoided for a reproducible roughness evaluation. Through a higher numerical aperture the critical angle of steep edges can be increased. Concerning white

light interferometers an adaptation of the evaluation algorithm of the interference figure can reduce the occurrence of batwings. The combined evaluation of peak and phase information of the interference figure reduces batwings significantly [9-11].

3.3 Small measuring fields

The increase of the numerical aperture is closely connected with an increase of the objective magnification and with that closely connected with a decrease of the measuring field size. To get a good compromise between an accurate measurement and large measuring fields a stitching with high numerical aperture objectives is necessary. Stitching is the recombination of successive, laterally displaced measurements to extend the measurement field for better statistically validated measurements.
With stitching two problems evolve. First a very accurate xy-stage is necessary. The reproducible lateral resolution of this xy-stage should be in the same range as the mechanical resolution of the microscope. The mechanical resolution d_m is the size of a CCD pixel d_{CCD} projected with the overall magnification M_A of the optical setup: $d_{CCD}= d_m M_A$. The cause for orienting the resolution of the xy-stage on the mechanical rather than the optical resolution [12] is the sensitivity of edge detections to lateral displacements [13]. Batwings occur on steep edges and as the round robin test showed batwings are like the steep edge detection very sensitive to lateral displacements, too.

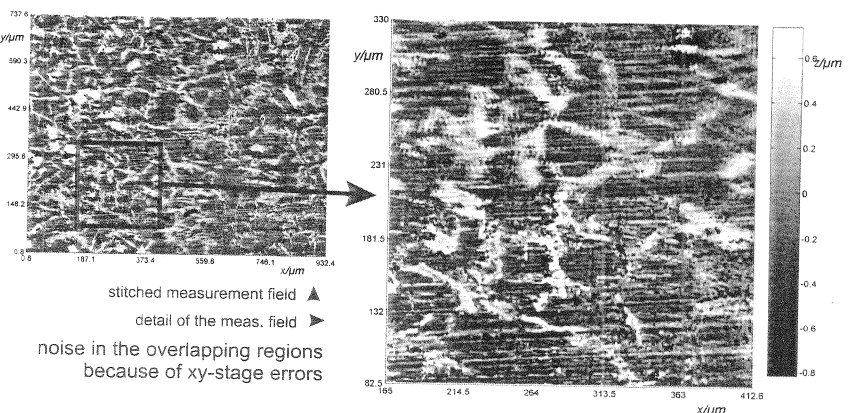

Fig.7: *stitched surface: lateral displacement and problems with the fitting of successive measurements lead to noise in the overlapping regions.*

The second problem with stitching is the necessity of having to fit the successive measurements into one big measuring field. This fit is mostly done using least square fitting algorithms which are sensitive to outliers. The least square fitting algorithms should be replaced through robust methods [14] yet to be developed, which are less sensitive to outliers.

4 Experiments

Commonly used roughness parameters in particular R_z show a significant variation if the same surface is measured with a tactile and an optical profiler. Reasons for these variations are various systematically differences, like interpolated missing points, batwings, and small measuring fields on the optical side and morphological filtering

through the stylus tip [15] and deformation of soft surfaces (aluminium) [16] on the tactile side. The common roughness parameters were developed for tactile systems based on experiences gathered over many years. Now with the development of 3D roughness parameters it is necessary to take the properties of both optical and tactile profilers into account and establish parameters that can be used with tactile and optical profilers. This can be realised with a structure oriented 3D roughness evaluation [5].
As can be seen in figure 8 the mean height of a structure is quite stable with varying optical systems. Some vertical calibration problems occurred with the confocal system B1 in measurements 2 and 3: the measured heights were too high. Similar vertical calibration problems are to be seen with two older white light interferometers A3 and F1: measurements 25 to 27 are too small. With measurements 10,11,14, and 15 it becomes clear that confocal microscopes have a problem with low numerical aperture objectives. With higher numerical apertures up to 0.8 the same microscope meets the reference height very good (measurements 18-22).

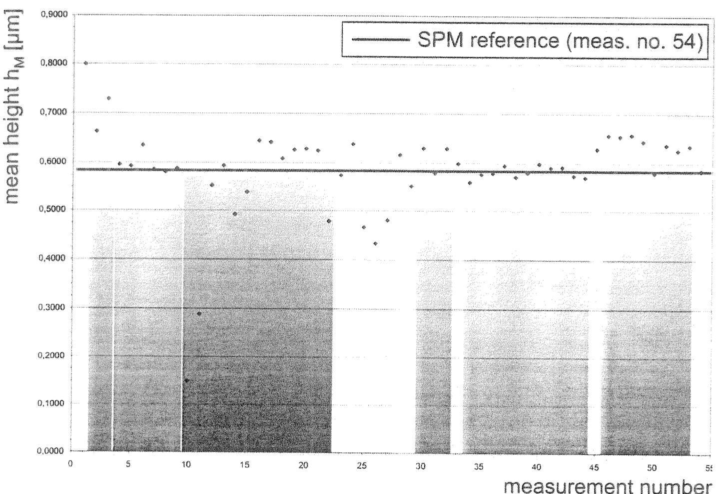

Fig.8: *mean height of the same crystal structure of a MMC surface measured with different optical profilers in different optical setups (please see appendix A1 for the precise optical setup of each measurement number).*

State of the art white light interferometers meet the reference height even with low numerical apertures. Measurements 33-53 show the two white light interferometer market leaders with different systems and different evaluation methods of the interference figure. Coherence peak (envelope) evaluation is done in measurements 33-45 and in measurement 50, phase evaluation with the rest of the measurements. The measurements with phase evaluation are a certain amount higher due to material effects: the structure is mainly made of silicon, the matrix is mainly made of aluminium. For this material combination Harasaki [17] proposes a height difference of approximately 40nm which is met quite well.
Figure 9 shows the five point height of the structure which is calculated in a comparable way to R_z. These heights vary heavily depending on the optical measurement system and its precise setup. The variation depends on systematic problems like batwings. With the five percent height h_{5P} (fig. 10) maximum values of a structure can be estimated without

being too dependent on the measurement system. Even the tactile reference measurement is met very well.
The calculation of the five percent height is based on the linear material ratio curve [18]. All detected structure points are sorted according to their height. Five percent of the highest points are dropped and the maximum height of the remaining points is the five percent height h_{5P} of the structure. This calculation is comparable to rank filters [19] like median (50% height), dilation (0% height) and erosion (100% height). It is also comparable to the 95th percentile without implying a normal distribution of the measured heights.

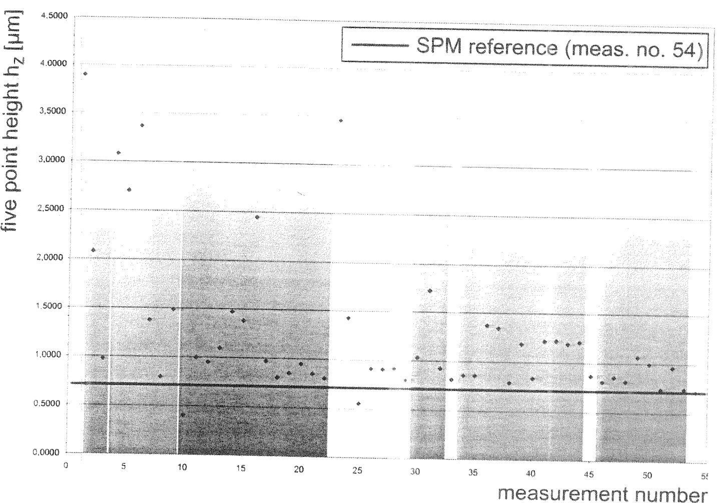

Fig.9: *five point height of the same crystal structure of a MMC surface measured with different optical profilers in different optical setups (please see appendix A1 for the precise optical setup of each measurement number).*

5 Conclusion

The round robin test revealed that optical measurements evaluated with common 2D roughness parameters are quite unstable due to systematic problems. But with an adaptation of the optical measuring conditions and the surface roughness parameters to the systematic differences of optical profilers a reproducible 3D roughness evaluation is possible.
The measuring conditions should be chosen in a way that batwings are suppressed. This can be realised with high numerical aperture objectives to rise the critical angle of steep edges. An additional phase evaluation of the interference figure of white light interferometers can reduce the amount of batwings, too.
A method to test a surface on steep critical edges is the successive measurement of the same surface area with a range of different objectives. The successive measurements are fitted into each other and if there occur significant height deviations between two objectives the objective with the higher numerical aperture has to be chosen. This quite complex test needs to be done only once to characterise a certain type of surface. This test is only feasible with white light interferometers because of the numerical aperture dependent height evaluation of confocal systems.

The analysis of the round robin test data showed further that a certain amount of optically measured points are unreliable. To reduce the unreliability of the optical data a lateral over sampling of the surface is necessary. Through statistical methods an identification of outliers is possible. For the estimation of the actual surface the additional information of adjacent measurement points can be used.
The subsequent signal processing of the measured surface should use robust algorithms to reduce the influence of outliers [14]. These robust methods also consider small amounts of missing points in a correct way. In general all filter algorithms should be prepared to deal with missing points without the necessity of a prior interpolation of the missing regions.

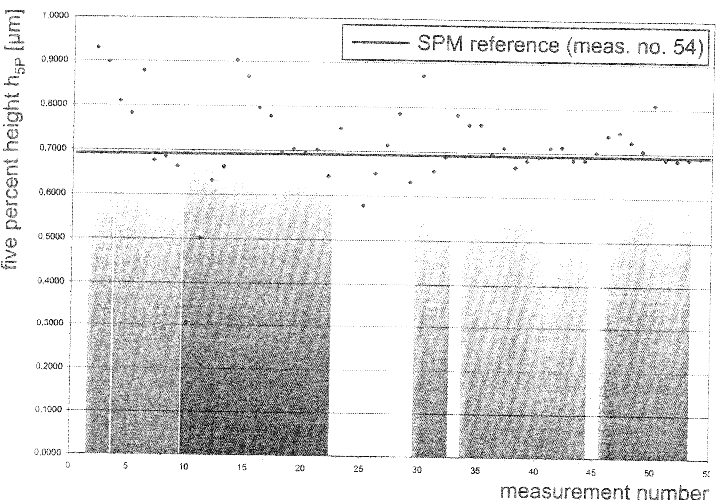

Fig.10: five percent height of the same crystal structure of a MMC surface measured with different optical profilers in different optical setups (please see appendix A1 for the precise optical setup of each measurement number).

By examining surface core regions a limited use of common 2D roughness parameters is possible. A 95% core region is a region in the vertical scale that contains 95% of the surface region points and has a minimal peak to valley height: $z_{max} - z_{min}$ -> minimize. The calculation of a standard deviation of this 95% core region provided stable results for the optical and even the tactile systems. Pre-condition is the removal of form and waviness of the evaluated region.
Due to systematic properties of optical profilers a reliable estimation of maximum and minimum values is impossible. These values provide only information about the measuring system and not about the measured surface. To get more stable information about the surface the use of adapted rank operators is necessary. The mentioned 5% height turned out to be quite independent from the measuring system and its optical setup, without dropping too much information of the measurement.

Acknowledgments

The authors would like to thank the *Arbeitskreis 3D-Rauheitsmesstechnik*: Audi AG: H. Lindner; BMW AG: E. Kindlein, M. Stiebler; DaimlerChrysler AG: Dr. N. Rau, T. Hercke; Dr.-Ing. h.c. F. Porsche AG: B. Burger; Federal Mogul GmbH: U. Lenhof; Volkswagen AG:

Dr. J. Strobel, Dr. U. Laudahn, C. Neukirch; Institut für Mess- und Regelungstechnik, Uni-Hannover: Prof. Dr. H. Bodschwinna, Dr. J. Seewig.

References

[1] T. Pfeifer, F. Bitte, G. Dussler, "*Optical metrology for Microsystems inspection*", Precision Engineering and Micro Technology, Proceedings of the International Seminar, pp. 39-52, 2000.
[2] H. Schwenke, U. Neuschaefer-Rube, T. Pfeifer, H. Kunzmann, "*Optical methods for dimensional metrology in production engineering*", Annals of the CIPR, vol. 51, no. 2, pp. 685-699, 2002.
[3] VDI2655-1, "*Optische Messtechnik an Mikrotopografien - Blatt 1.1: Kalibrieren von Interferenzmikroskopen und Tiefeneinstellnormalen für die Rauheitsmesstechnik*", Düsseldorf, 2004.
[4] G. Dai, F. Pohlenz, U. Danzebrink, H. R. Krüger-Sehm, K. Hasche, "*Metrological scanning force microscopy applicable for surface evaluation*", ICS, Internat. Colloquium on Surfaces, 11. Internat. Oberflächenkolloquium, Part 2, vol. 11, pp. 1-10, 2004.
[5] A. Weidner, J. Seewig, H.-W. Lemke, "*Structure oriented parameters for the function related evaluation of data for 3D surface roughness*", ICS, Internat. Colloquium on Surfaces, 11. Internat. Oberflächenkolloquium, vol. 11, pp. 233-241, 2004.
[6] A. Weidner, J. Seewig, and E. Reithmeier, "*Structure oriented 3D roughness evaluation with optical profilers*", 10th Conference "Metrology and Properties of Engineering Surfaces", to be published, 2005.
[7] J. Schmit, A. Harasaki, "*High precision interferometric shape measurement of objects with areas of different reflectance*", Proceedings of SPIE - Metrology-based Control for Micro-Manufacturing, vol. 4275, pp. 85-93, 2001.
[8] A. Harasaki, J. C. Wyant, "*Fringe modulation skewing effect in white-light vertical scanning interferometry*", Applied Optics, vol. 39, no. 13, pp. 2101-6, 2000.
[9] P. de Groot, X. Colonna de Lega, J. Kramer, M. Turzhitsky, "*High precision surface inspection on the microscale by broadband interferometry*", Fringe 2001, 4th International Workshop on Automatic Processing of Fringe Patterns, Bremen, pp. 47-55, 2001.
[10] J. Schmit and G. Olszak, A, "*Some challenges in white light phase shifting interferometry*", Proceedings of SPIE - Interferometry XI: Techniques and Analysis, vol. 4777, pp. 118-127, 2002.
[11] A. Harasaki, J. Schmit, and J.C. Wyant, "*Improved vertical-scanning interferometry*", Applied Optics, vol. 39, no. 13, pp. 2107-2115, 2000.
[12] M. Born and E. Wolf, "*Principle of Optics - Electromagnetic Theory of Propagation, Interference and Diffraction of Light*". Pergamon Press, fifth ed., 1975.
[13] B. S. Lee, T. C. Strand, "*Profilometry with a coherence scanning microscope*", Applied Optics, vol. 29, no. 26, pp. 3784-3788, 1990.
[14] S. Brinkmann and H. Bodschwinna, "*Advanced Gaussian Filters*", Advanced techniques for assessment surface topography: development of a basis for 3D surface texture standards "SURFSTAND", (L. Blunt and X. Jiang, eds.), pp. 62-90, London: Kogan Page Science, 2003.
[15] M. Krystek, "*Morphological filters in surface texture analysis*", XI. International Colloquium on Surfaces, Proceedings Part 1, vol. 11, pp. 43-55, 2004.
[16] O. Kranz, "*Untersuchungen des Abtastvorganges bei der Rauheitsmessung*", PhD thesis, University of Hannover, 1980.
[17] A. Harasaki, J. Schmit, and J. C. Wyant, "*Offset of coherent envelope position due to phase change on reflection*" Applied Optics, vol. 40, no. 13, pp. 2102-2106, 2001.
[18] ISO13565-2, "*Geometrical Product Specifications (GPS) - Surface texture: Profile method; Surfaces having stratified functional properties - Part 2: Height characterization using the linear material ratio curve*" Geneve, Switzerland, 1996.
[19] P. Soille, "*Morphological Image Analysis: Principles and Applications*", Berlin: Springer, 1999.

Appendix A1

Meas.No.	Manufacturer	Meas.Sys.	Principle	Algorithm	Objective	NA	xScale [µm]	yScale [µm]		hM [µm]	hZ [µm]	h5P [µm]
1	A	1	CONF	CM	20	0,45	0,9125	0,9125		0,7998	3,8992	2,0721
2	B	1	CONF	CM	20	0,5	0,7813	0,7813		0,6629	2,0816	0,9302
3	B	1	CONF	CM	50	0,8	0,3125	0,3125		0,7289	0,9758	0,8983
4	B	2	CONF	CM	20	0,5	0,0914	0,0914		0,5954	3,0795	0,8099
5	B	2	CONF	CM	20	0,5	0,3662	0,3662		0,5927	2,7022	0,7825
6	B	2	CONF	CM	20	0,5	0,1701	0,1701		0,6352	3,3671	0,8783
7	B	2	CONF	CM	50	0,8	0,1465	0,1465		0,5859	1,3711	0,6768
8	B	2	CONF	CM	50	0,8	0,1465	0,1465		0,5812	0,7973	0,6854
9	B	2	CONF	CM	50	0,8	0,0837	0,0837		0,5881	1,4864	0,6635
10	C	1	CONF	CM	20	0,46	1,4883	1,4063		0,1497	0,4108	0,3058
11	C	1	CONF	CM	20	0,46	1,4883	1,4063		0,2889	0,9969	0,5022
12	C	1	CONF	CM	50	0,8	0,6250	0,5898		0,5532	0,9520	0,6322
13	C	1	CONF	CM	50	0,8	0,6250	0,5898		0,5939	1,0943	0,6631
14	C	1	CONF	CM	20	0,46	1,5625	1,5078		0,4919	1,4720	0,9031
15	C	1	CONF	CM	20	0,46	1,5625	1,5078		0,5395	1,3774	0,8658
16	C	1	CONF	CM	50	0,5	0,6250	0,6016		0,6447	2,4458	0,7957
17	C	1	CONF	CM	50	0,5	0,6250	0,6016		0,6417	0,9703	0,7772
18	C	1	CONF	CM	50	0,8	0,6250	0,6016		0,6086	0,8070	0,6965
19	C	1	CONF	CM	50	0,8	0,6250	0,6016		0,6265	0,8528	0,7039
20	C	1	CONF	CM	50	0,8	0,6250	0,6016		0,6284	0,9459	0,6954
21	C	1	CONF	CM	50	0,8	0,6250	0,6016		0,6247	0,8507	0,7027
22	C	1	CONF	CM	50	0,8	0,3125	0,3125		0,4786	0,8063	0,6433
23	D	1	CONF	MI	20	0,5	0,2860	0,2860		0,5748	3,4557	0,7511
24	E	1	CHROM	CM	0	0,5	1,0050	1,0050		0,6383	1,4227	0,9702
25	A	3	WLI	Env	10	0,25	3,6765	3,8235		0,4660	0,5540	0,5781
26	A	3	WLI	Env	20	0,4	1,8382	1,9118		0,4334	0,9094	0,6506
27	F	1	WLI	Env	20	0,4	0,5860	0,5860		0,4806	0,9064	0,7141
28	A	2	WLI	Phase	10	0,3	1,2846	1,2846		0,6163	0,9157	0,7851
29	A	2	WLI	Phase	20	0,4	0,6461	0,6461		0,5525	0,8043	0,6309
30	G	1	WLI	Phase	10	0,3	1,7578	1,7779		0,6301	1,0313	0,8709
31	G	1	WLI	Env	50	0,55	0,3516	0,3610		0,5792	1,7288	0,6569
32	G	1	WLI	Phase	50	0,55	0,3516	0,3610		0,6293	0,9246	0,6884
33	H	3	WLI	Env	10	0,3	1,9275	1,6519		0,5991	0,8149	0,7831
34	H	1	WLI	Env	5	0,13	1,6471	1,9219		0,5606	0,8597	0,7612
35	H	1	WLI	Env	5	0,13	1,6471	1,9219		0,5767	0,8602	0,7616
36	H	1	WLI	Env	20	0,4	0,4116	0,4802		0,5791	1,3707	0,6966
37	H	1	WLI	Env	20	0,4	0,4116	0,4802		0,5947	1,3444	0,7109
38	H	1	WLI	Env	20	0,4	0,8251	0,9628		0,5717	0,7911	0,6671
39	H	1	WLI	Env	20	0,4	0,4116	0,4802		0,5802	1,1844	0,6818
40	H	1	WLI	Env	20	0,4	0,8251	0,9628		0,5983	0,8388	0,6904
41	H	1	WLI	Env	50	0,55	0,1638	0,1911		0,5910	1,2153	0,7111
42	H	1	WLI	Env	50	0,55	0,1638	0,1911		0,5917	1,2191	0,7132
43	H	1	WLI	Env	50	0,55	0,3284	0,3832		0,5739	1,1894	0,6837
44	H	1	WLI	Env	50	0,55	0,3284	0,3832		0,5704	1,2079	0,6839
45	H	2	WLI	Env	20	0,4	0,8211	0,9581		0,6285	0,8687	0,7017
46	K	1	WLI	Phase	5	0,13	2,2447	2,2447		0,6562	0,8102	0,7389
47	K	1	WLI	Phase	10	0,3	1,1122	1,1122		0,6542	0,8572	0,7467
48	K	1	WLI	Phase	20	0,4	0,5574	0,5574		0,6574	0,8156	0,7254
49	K	1	WLI	Phase	50	0,55	0,2377	0,2377		0,6442	1,0664	0,7056
50	K	1	WLI	Env	10	0,3	1,6733	1,6733		0,5800	0,9936	0,8089
51	K	1	WLI	Phase	10	0,3	2,2642	2,2642		0,6367	0,7391	0,6866
52	K	1	WLI	Phase	50	0,55	0,5694	0,5694		0,6258	0,9604	0,6842
53	K	1	WLI	Phase	50	0,55	0,5694	0,5694		0,6347	0,7424	0,6875
54	PTB	M-LRSPM	SPM				0,5000	0,5000		0,5846	0,7164	0,6910

Tab.1: *setup of the optical profilers with measurement data; Principle: CONF – confocal microscope, CHROM – chromatic sensor, WLI – white light interferometer, SPM – scanning probe microscope; Algorithm: CM – centre of mass, MI – maximum intensity, Env – coherence Peak / Envelope of the interference figure, Phase – phase evaluation of the figure.*

SESSION II

JULY 5, 2005

CHARACTERISATIONS I

(SCALE EFFECTS)

CHAIRMAN
Prof. T.THOMAS

Identification of Manufacturing Signature by 2D Wavelet Decomposition — *Page 61*
Hassan ZAHOUANI, Saber MEZGHANI, Roberto VARGIOLU, Michel DURSAPT

Multiscale analysis of roughness measurements: the Scale Pertinence — *Page 69*
Maxence BIGERELLE, Adrien VAN GORP, Alain IOST

Surface Influence on the Behavior of Rolling Body — *Page 81*
ROSCA Ileana

Linear Feature Extraction Based on Complex Ridgelet Transform — *Page 85*
Xiangqian JIANG, Wenhan ZENG, Paul SCOTT, Jianwei MA, Liam BLUNT

Application of a wavelet transform for multifractal image analysis of rough surfaces characterization and classification — *Page 93*
Saber MEZGHANI, Hassan ZAHOUANI